Arabian Journal of Chemistry (2020) 13, 2483–2495

King Saud University

Arabian Journal of Chemistry

www.ksu.edu.sa
www.sciencedirect.com

ORIGINAL ARTICLE

CuNPs decorated molecular imprinted polymer on MWCNT for the electrochemical detection of L-DOPA

M.P. Sooraj [a], Archana S. Nair [a], Suresh C. Pillai [b,c], Steven J. Hinder [d], Beena Mathew [a,*]

[a] *School of Chemical Sciences, Mahatma Gandhi University, Kottayam 686560, Kerala, India*
[b] *Nanotechnology and Bio Engineering Research Group, Department of Environmental Sciences, Institute of Technology Sligo, Ireland*
[c] *Centre for Precision Engineering, Materials and Manufacturing Research, Department of Environmental Science,Institute of Technology Sligo, Ash Lane, Sligo, Ireland*
[d] *The Surface Analysis Laboratory, Department of Mechanical Engineering Sciences, University of Surrey, Guildford, Surrey GU2 7XH, UK*

Received 24 March 2018; accepted 3 June 2018
Available online 22 June 2018

KEYWORDS

Electrochemical sensor;
Molecular imprinted polymer;
MWCNT;
Copper nanoparticle;
L-DOPA

Abstract A novel synthesis of copper nanoparticle (CuNPs) is carried out by the reduction of ethylene diamine Cu complexes using sodiumborohydride as reducing agent. The synthesized copper nanoparticle is grafted with molecular imprinted polymer on MWCNT (CuNPs/MWCNT-MIPs). Fabricated sorbent is used for the molecular recognition and sensing of levodopa (L-DOPA) in human urine and pharmaceutical samples. The non covalent interaction between L-DOPA and the functional groups present in the selective binding sites of the polymer composite sorbent is mainly responsible for the recognition property. The synthesis of CuNPs decorated MWCNT-MIPs and its extents are characterized by employing UV–Vis spectroscopy, Fourier-transform infrared spectroscopy, powder X-ray diffraction analysis, X-ray photoelectron spectroscopy, scanning electron microscopy and transmission electron microscopy techniques. The electrochemical investigation shows that the imprinted (CuNPs/MWCNT-MIP) material has good recognition capacity towards L-DOPA. The sensitivity is found to be directly proportional to the concentration of template with a detection limit of 7.23×10^{-9}M (S/N = 3). The specificity

* Corresponding author.
E-mail address: beenamathew@mgu.ac.in (B. Mathew).
Peer review under responsibility of King Saud University.

Production and hosting by Elsevier

https://doi.org/10.1016/j.arabjc.2018.06.002

and selectivity of the fabricated sensor give a fine discrimination between L-DOPA and structurally related compounds such as dopamine, uric acid, 3,4-Dihydroxyphenylacetic acid and homovanillic acid.

1. Introduction

L-DOPA (levodopa) is the precursor to various neurotransmitters collectively known as catecholamines. It is considered as an excellent drug for the treatment of Parkinson's disease by many clinicians (Brooks, 2008; Jankovic, 2008). The biomedical significance of the drug has induced the development of various analytical techniques for the quantification of both the stereo isomers of DOPA and its precursors. It is essential to monitor the quantity of L-DOPA in its dosage forms, as it is suddenly oxidised if in contact with air or moisture, which leads to drug loss and potency reduction (Carstensen, 1990). Many methods including HPLC (Török et al., 2006; Dhanani et al., 2015; Mc Murtrey et al., 2000), CE (Mc Evoy, 2006; Wei et al., 2007) etc. has been reported for the quantification of levodopa in its dosage forms. Most of these reported methods have drawbacks such as poor selectivity and sensitivity. It should be noted that some of the methods have shown high sensitivities and selectivity towards the drug. However they are expensive and require longer analysis time. The fabrication of a system for the quantification of L-DOPA in its dosage forms overcoming these drawbacks was the main aim of this work.

Molecular imprinted polymer based electrochemical sensor is one of the method that overcomes these difficulties. Recently, huge quantum of work has been reported in the field of electro chemical detection of biomolecules (Roy et al., 2014; Kong et al., 2012; Afkhami et al., 2013; Yang et al., 2014). MWCNTs are composed of rolled 2D graphene sheets which attain a nano tubular morphology having higher surface to volume ratio (Rashid et al., 2012), high electrical (Menghe, 2011) and thermal conductivity (Kim et al., 2007) and chemical stability. They have the capability to speed up electron transfer and maximize the sorption ability of electroactive probe on the surface of the electrode, then strengthen the electrochemical signals (Saleh et al., 2009). Because of the greater conductivity, compatibility and surface enhanced Raman scattering ability, the CuNPs have drawn the consideration of researchers to be used as a crucial component for clubbing with carbon nanotubes (Sulekh et al., 2014). It was also demonstrated that CuNP/CNT composite had environmental stability, better durability and electrical and thermal conductivity than those of the individual materials alone (Hyun et al., 2015). The clubbing of nanomaterials with distinctive properties of MIPs can improve their performance as electrochemical sensors. Metal nanoparticles like CuNPs and MWCNT offer better accessibility of the template molecule to the imprinted sites and improve the sensitivity as well as detection limits.

In the present study, the synthesis and applications of CuNPs/MWCNT-MIPs modified glassy carbon electrode (GCE) for the sensing of L-DOPA in tablets, and spiked human urine samples have been elaborated. The CuNPs/MWCNT-MIPs were fabricated by taking L-DOPA as template, acrylamide as functional monomer, ethylene glycol dimethacrylate as cross-linker and 2,2′-azo-bisisobutyronitrile as initiator. The adsorption experiments were used to study the selective recognition of CuNPs/MWCNT-MIP towards L-DOPA. The product and intermediates produced during the construction of CuNPs/MWCNT-MIPs were analyzed using UV–vis. spectroscopy, Fourier-transform infrared spectroscopy, thermogravimetric analysis, powder x-ray diffraction technique and X-ray photoelectron spectroscopy analyses and their morphologies were observed by scanning electron microscopy and transmission electron microscopic techniques. The fabricated sensing material shows many advantages like low detection limit, fast response, ease of application and cost-effectiveness. In our belief, the method proposed in this work would be a probable breakthrough in the efficient electrochemical determination of L-DOPA in biological fluids and pharmaceutical samples.

2. Materials and methods

2.1. Chemicals and reagents

All reagents used in the present work were of analytical grade. Multiwalled carbon nanotubes were purchased from Reinste Nano Ventures Private Limited, India. $CuSO_4{\cdot}5H_2O$, acrylamide (AAm, 98%), allyl alcohol (AA 99%), ethylene glycol dimethacrylate (EGDMA, 98%) and all other solvents were obtained from Merck, India. L-DOPA (99%), dopamine hydrochloride (DA, 99%), uric acid (UA), 3,4-Dihydroxyphenylacetic acid (DOPAC, 99%), homovanillic acid (HVA, 99%), 2,2′-azo-bisisobutyronitrile (AIBN), thionyl chloride ($SOCl_2$), Na_2HPO_4 and NaH_2PO_4 required for the preparation of sodium phosphate-buffer solution (PBS, pH 7.0) were obtained from Sigma Aldrich. Distilled water was used throughout the experiment. All chemicals and solvents were used as received without further purification.

2.2. Apparatus and equipment

Electrochemical measurements were performed with Biologic SP-200 Science instrument. A three-electrode system was used for cyclic voltammetric (CV) and differential pulse voltammetric (DPV) analysis. CuNPs/MWCNT-MIPs modified glassy carbon electrode (GCE) was used as the working electrode, a saturated calomel electrode (SCE) and a platinum wire was used as the reference and counter electrode respectively. The Fourier-transform infrared (FT-IR) spectra were recorded on a Perkin-Elmer 400 FT-IR spectrophotometer. UV–vis. absorption spectra were investigated by a Shimadzu UV vis. spectrophotometer model 2450. Thermogravimetric analysis (TGA) was conducted on a NETZSCHSTA449C instrument from room temperature to 700 °C. The crystalline nature of the synthesized products and intermediates were recorded on Pan Analytic Expert-Pro-Anal PXRD instrument (PXRD).

X-ray photoelectron spectroscopy (XPS) spectra were acquired using a Thermo Fisher K-Alpha$^+$ spectrometer. Morphological images of pure MWCNT and surface modified MWCNT were recorded on a JEOL-JSM-6390A scanning electron microscope (SEM) and JEOL-2100 transmission electron microscope (TEM).

2.3. Preparation of copper nanoparticle (CuNPs)

The CuNPs were synthesized through reduction of ethylenediamine copper complex using sodium borohydride as a reducing agent. Ethylenediamine copper complex was prepared by sonicating 1 M $CuSO_4{\cdot}5H_2O$ and 2 M ethylenediamine in 25 mL deionised water for about 3 min. To this solution, 75 mL of 0.25 M $NaBH_4$ solution is added with 3.5 g starch as a stabilizing agent dropwise at ambient temperature. The color of the solution changes from blue to dark brown confirming the formation of CuNPs (Fig. 1). The sythesised nanoparticle is separated by centrifuging at 14,000 rpm and washing repeatedly with deionised water followed by drying under vacuum.

2.4. Preparation of vinyl functionalized MWCNT (MWCNT-CH = CH_2)

Vinyl functionalized MWCNTs were synthesized via a three-step process. The preliminary step was the carboxylation of MWCNTs. For this, 0.75 g MWCNT was taken in an RB flask and conc. H_2SO_4 and HNO_3 in the ratio 3:1 was added. The reaction mixture was allowed to reflux at about 80 °C for 18 h under vigorous stirring. After acid treatment, the reaction mixture was diluted with deionised water and filtered through 0.2 μm PTFE membrane to separate the solid component. The washing was repeated until the pH of the filtrate became neutral. The solid substance was dried under vacuum at 65 °C for 12 h, yielding MWCNT-COOH. The next step was the conversion of MWCNT-COOH to MWCNT-COCl using thionyl chloride. About 0.75 g MWCNT-COOH and 15 mL $SOCl_2$ in 20 mL THF were taken in a reaction vessel and heated at 70 °C for 18 h under vigorous stirring. The mixture was then repeatedly washed with THF (250 mL). The product was separated by centrifugation at 16,000 rpm and dried under vacuum at 65 °C for 12 h. Final step was the vinyl functionalisation of the obtained MWCNT-COCl. For this, 4 mL allyl alcohol and 2 mL pyridine were mixed with the acid chloride functionalised MWCNTs (200 mg) dispersed in 15 mL of THF. The components were sonicated for about1h at room temperature under nitrogen atmosphere. The resultant solid was filtered, washed with THF, and dried in a vacuum oven at 50 °C overnight.

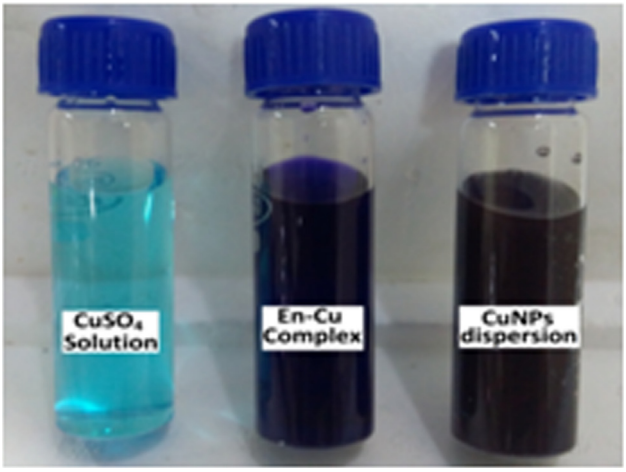

Fig. 1 The colour change during the synthesis of CuNPs (Light blue-dark blue/violet-brown/black).

2.5. Synthesis of CuNP decorated levodopa (L-DOPA) imprinted and non imprinted polymer on MWCNT (CuNPs/MWCNT-MIPs/NIPs)

For the synthesis of CuNPs decorated molecular imprinted polymer on MWCNT, initialy 150 mg of MWCNTCH = CH_2 and 25 mg of CuNPs were dispersed in 25 mL DMF in a reaction flask and kept under ultrasonic vibration for 30 min. To this 0.5 mmol of L-DOPA, 4 mmol of AAm and 1 mmol of EGDMA were added followed by sonication for about 10 min. under N_2 atmosphere. Then 50 mg of radical initiator AIBN was added and the mixture was allowed to polymerize for 24 h at 70 °C. The final product was separated by filtration and the template molecule on the polymer matrices were removed by continuous washing with DMF and then dried under vacuum. The non imprinted polymer was synthesized using the same method but only in the absence of L-DOPA.

2.6. Electrochemical experiments

Prior to surface modification, the GCE was polished with 0.05 μm alumina slurries followed by washing with deionised water, and then sonicated in 50% nitric acid, 1 M NaOH, and finally in water. The CuNPs/MWCNT-MIPs or NIPs (20 mg) were dispersed in 0.5 mL acetone by ultrasonication for about 5 min. The dispersed medium was coated on a clean GC electrode surface by drop casting and dried under IR lamp for about 1 h. 0.1 mL of 1% (w/v) nafion solution was coated on the above GCE till the complete gelling (Scheme 2). After drying, the CuNPs/MWCNT-MIP modified GCE was incubated in a known concentration of L-DOPA solution. After careful rinsing with deionised water, the modified GCE was transferred into fresh PBS (0.1 mol L^{-1} pH 7) solution for detailed electrochemical studies. CV was recorded with a scan rate of 100 mV s^{-1} from −1000 mV to +1000 mV for L-DOPA. DPV analysis was done in the potential range of 0 to 600 mV with a scan rate of 20 mV s^{-1}, a pulse amplitude 50 mV, and a pulse width of 50 ms to monitor the current response of L-DOPA. The kinetic behavior of the sensor towards L-DOPA was also monitored. The sensor was immersed in 1×10^{-6} mol L^{-1} L-DOPA solution with equilibration for 1, 2, 3, 4, 5, 7 and 9 min at room temperature. After each incubation period, the modified GCE was carefully washed with deionised water, to keep away from carryover L-DOPA. The electrode was then transferred into 0.1 mol L^{-1} PBS (pH 7.0) and the differential pulse voltammograms were recorded.

3. Results and discussion

3.1. Spectral and morphological characterization

UV–Visible absorption spectra of the synthesized CuNPs are shown in Fig. 2. The spectrum shows a strong absorption peak around 635–645 nm because of surface plasmon band of Cu colloids (Annu et al., 2011; Sukalyan et al., 2008; Vincenzo et al., 2009). The strong surface plasmon band with absorption maxima at 640 nm due to the collective oscillation of conduction electrons at the surface confirms the formation of CuNPs.

FT-IR spectra of MWCNT, functionalized MWCNT and CuNPs/MWCNT-MIP before and after leaching out L-DOPA from the polymer matrices are compared (Fig. 3) and it confirms the proposed binding mechanism of non covalent interaction between the template and polymer sorbent (scheme 1). In the spectrum (a) purified MWCNT (Rike et al., 2011) showed peaks at 1737 and 2928 cm^{-1} characteristic of C═O stretching vibration and the asymmetric C—H stretching vibration respectively. In (b) acid processed MWCNTs displayed the characteristic stretching peaks of –OH and —CO groups of carboxylic acid at 3300 and 1581 cm^{-1} respectively (Mohamed et al., 2017). The peak at 1352 cm^{-1} could be attributed to the C—O stretching vibrations of —COOH. A strong peak associated with ester linkage around 1234 and 1103 cm^{-1} (C—O stretching vibration of symmetric and asymmetric ester) was observed in (c), the presence of which suggests that allyl alcohol is coupled to MWCNT through ester linkage. The sorbent with and without L-DOPA gave a very notable change in their spectra. The appearance of an additional broad peak in the region 3436 cm^{-1} corresponding to the- OH stretching of L-DOPA in the spectrum of CuNPs/MWCNT-MIP before template removal (e) conveys the successful embedding of L-DOPA within the polymer matrix during the imprinting process.

X-ray diffraction patterns (Fig. 4(A) and (B)) of (a) pristine and (b) vinyl functionalized MWCNTs shows two characteristic crystalline peaks of MWCNT (Masooma et al., 2015) at 2θ values 25.6° and 43.6° corresponding to the interlayer spacing (d_{002}) and reflection (d_{100}) respectively. In the case of synthesized CuNPs (c) well defined peaks corresponding to (1 1 1),

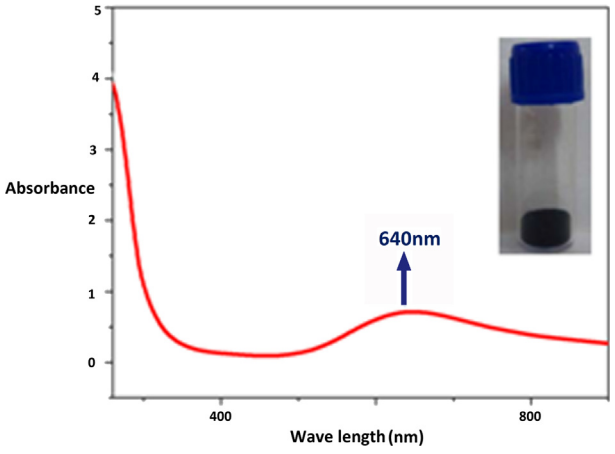

Fig. 2 UV–visible absorption spectrum of the synthesized CuNPs by the reduction of ethylenediamine copper complex.

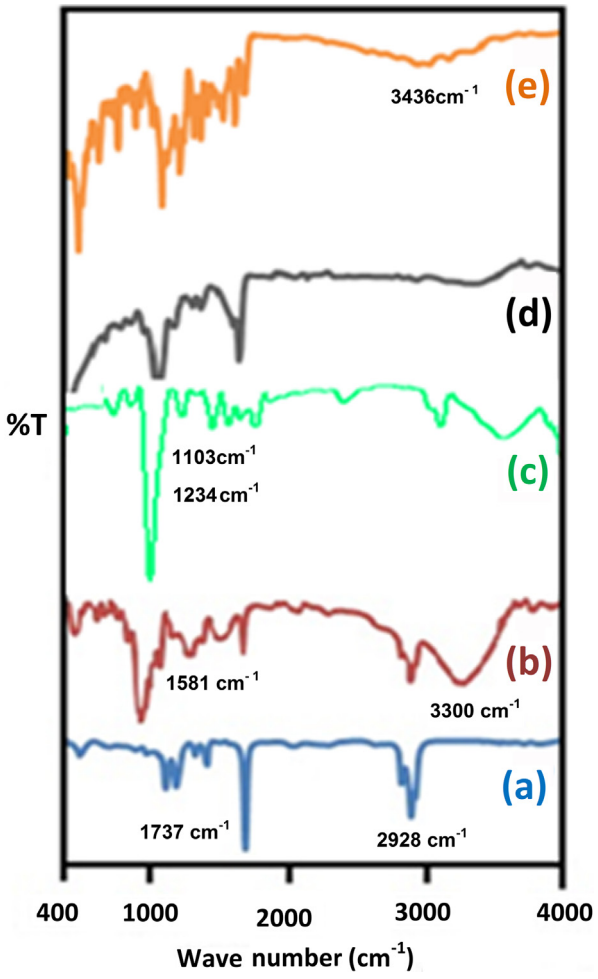

Fig. 3 FTIR spectra of (a) purified MWCNT, (b) MWCNT-COOH, (c) MWCNT-CH═CH_2, (d) CuNPs/MWCNT-MIPs without L-DOPA and (e) CuNPs/MWCNT-MIPs with L-DOPA.

(2 0 0), and (2 2 0) of CuNPs were observed and this confirms the formation of CuNPs (Bharat et al., 2013. Jungsup et al., 2017). The spectrum also shows the peaks (2 2 0) and (1 1 1) corresponding to Cu_2O nanoparticle (André et al., 2009; Ayesha et al., 2016) because the separation, purification and characterization process of nanoparticles were done in normal atmospheric condition ie, in the presence of O_2. In CuNP/MWCNT-MIP, the sorbent shows the characteristic crystalline peaks corresponding to CuNPs in addition to the peaks of CuNP/MWCNT-MIP, giving an idea that the CuNPs were effectively grafted on CuNP/MWCNT-MIP.

The SEM micrographs shows the morphological differences of MWCNT, CuNPs, CuNPs/MWCNT-CH═CH_2 and the CuNPs/MWCNT-MIP (Fig. 5). The MWCNT showed nano-sized tubular structure with almost similar diameter (6–8 nm). The synthesized CuNPs showed average diameter within the nano range 20–35 nm. The images of CuNPs/MWCNT-CH═CH_2 showed tubular forms decorated with small shapes of CuNPs. It confirms the grafting of CuNPs on the surface of MWCNT-CH═CH_2 during the synthesis. The CuNPs/MWCNT-MIP retains the tubular morphology with increase in thickness and the images give an idea that the polymer is wrapped on CuNPs during the CuNP/MWCNT-MIP

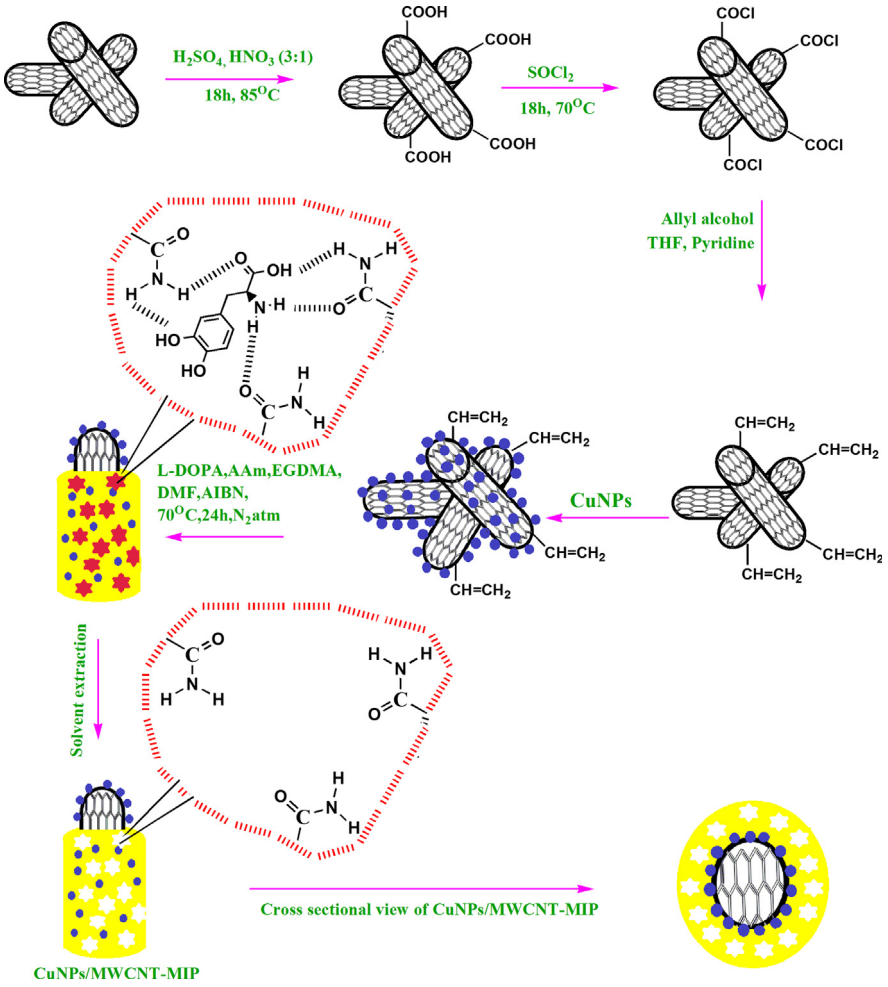

Scheme 1 Synthesis route of CuNPs/MWCNT-MIP.

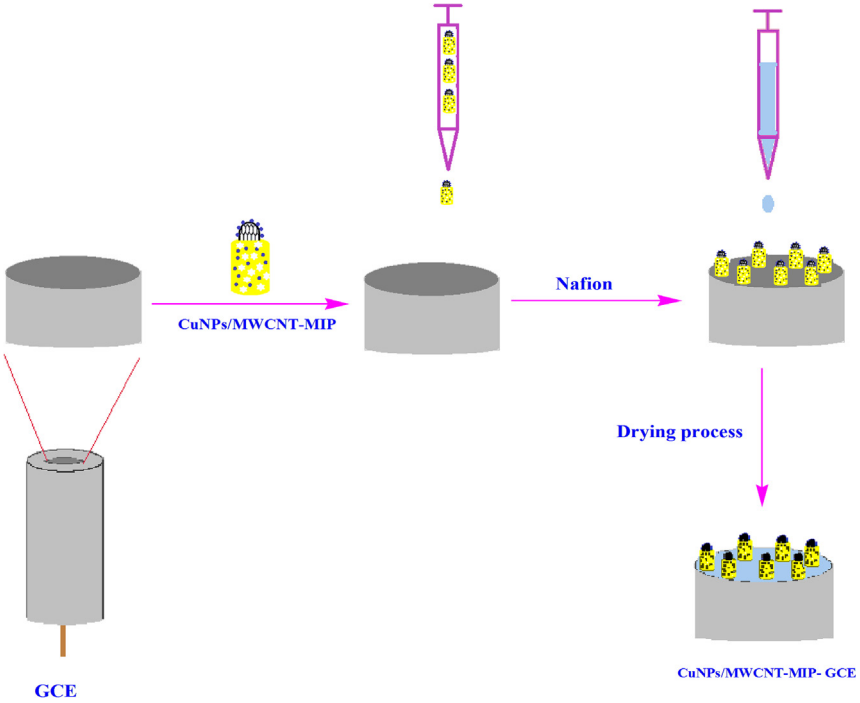

Scheme 2 Schematic representation of the construction of CuNPs/MWCNT-MIP on GCE.

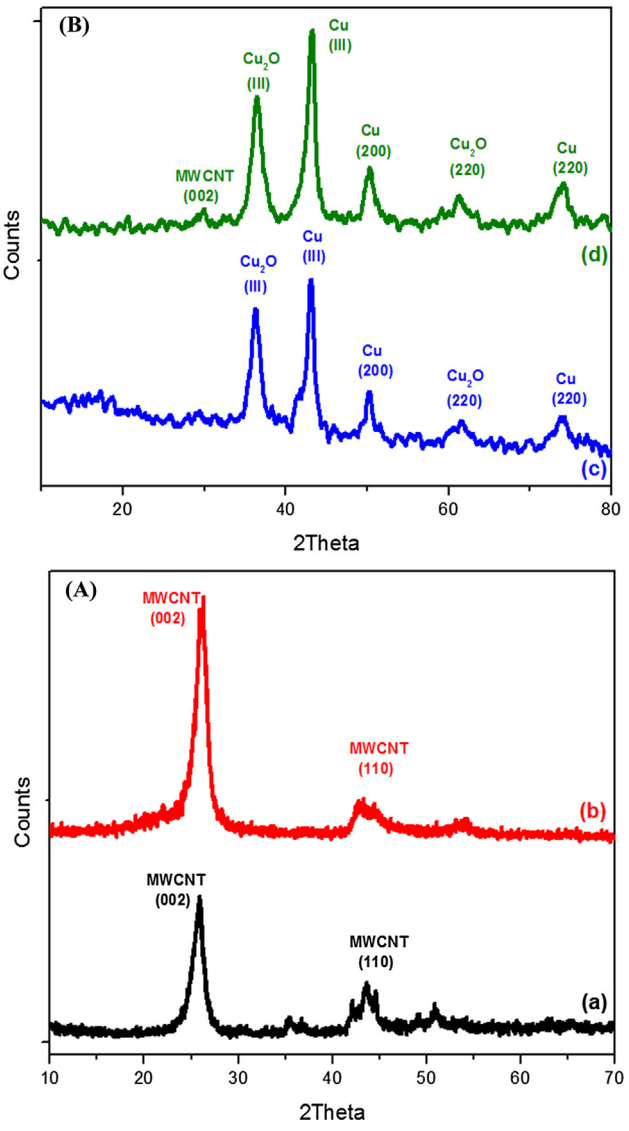

Fig. 4 (A) and (B) Powder X-ray diffraction patterns of (a) MWCNT, (b) MWCNT-CH═CH_2 (c) CuNPs (d) CuNPs/MWCNT-MIP.

preparation. CuNPs/MWCNT-MIP shows rough surface morphology due to the cavities formed during the time of extraction of template molecules from the surface of the sorbent. The morphologies were further studied by TEM analysis.

The TEM images (Fig. 6) indicate the morphological differences between the pristine MWCNT, CuNPs and CuNP/MWCNT-MIP. TEM images of pristine MWCNTs confirm the tubular morphology (diameter 6–8 nm and length of some micrometers). The TEM morphology of CuNPs gives information about the visual appearance and particle size (diameter). The TEM analysis confirms that synthesized CuNPs having diameter about 30–35 nm. The SAED image of CuNPs exhibits the distinct diffractions of both Cu (0) and Cu (II) nanoparticles (Debart et al., 2001). The sorbent CuNPs/MWCNT-MIP shows the tubular morphology like MWCNT but with an increase in diameter to about 70–80 nm. It is due to the formation of MIP on the surface of the CuNPs/MWCNT-CH═CH_2. Also the image clearly shows the presence of CuNPs on MIP without changing the innate tubular morphology of carbon nanotube.

The presence of CuNPs on CuNPs/MWCNT-MIP was monitored by XPS analysis (Fig. 7). The survey spectrum in Fig. 7a shows distinct peaks for copper, carbon, oxygen and nitrogen at 933, 285, 531.2 and 400 eV respectively. From the high resolution spectra in Fig. 7b–e the concentrations (in atomic %) of carbon (61.75 at.%), copper (5.24 at.%), oxygen (22.72 at.%) and nitrogen (22.72 at.%) were calculated. The XPS of Cu 2p (Fig. 5(b)) shows four distinct peaks, the Cu $2p_{3/2}$ peak at 933.1 eV is characteristic of copper in the +2 oxidation state and the peaks at 943.7 eV is a $Cu2p_{3/2}$ shake-up satellite (Akhavan et al., 2011). The peaks at 953.1 and 963.1 eV, are the $Cu2p_{1/2}$ peak and its shake-up satellite peak respectively (Leite et al., 2012).

Fig. 8 shows the TGA curves of purified MWCNT, MWCNT-CH═CH_2 and CuNPs/MWCNT-MIPs and conventional MIP. Purified MWCNT was found to be stable up to 700 °C. The TGA pattern of vinyl functionalized MWCNT have a continuous but not obvious mass loss due to the thermal degradation of —CH═CH_2 functional groups attached to the surface of MWCNT. The TGA pattern of CuNPs/MWCNT-MIPs has an almost similar degradation pattern of conventional MIP. However, the temperature at which the initial degradation start increased after the grafting of CuNPs decorated MWCNT on to MIP. This result suggests that the grafting of nanomaterials on to the MIP will increase the thermal stability to the polymer matrix. From the non decomposed mass of CuNPs/MWCNT-MIPs percentage of nanostructures in it was found to be about 20%.

3.2. Electrochemical behavior of the CuNPs/MWCNT-MIP/NIPs modified GCE

The Fig. 9 shows the CV of 1×10^{-5} mol L^{-1} L-DOPA in PBS (0.1 mmol L^{-1}, pH 7.0) obtained using CuNPs/MWCNT-MIP coated GCE. The cyclic voltagram of L-DOPA on CuNP/MWCNT-MIP coated GCE shows a peak at 243 mV (peak 1) because of the electro oxidation of L-DOPA to dopaquinone. During reverse scan, a peak 2 corresponding to the reduction of dopaquinone was observed at 202 mV but the peak current was decreased very much. Another two redox peaks at -300 mV (peak3) and −154 mV (peak 4) were observed during the initial and subsequent scans. The cathodic peak 3 and anodic peak 4 correspond to the oxidation of cyclodopa (CD) to dopachrome (DC) and the reduction of DC to CD respectively. The mechanism of the electro oxidation is shown in the Scheme 3.

To confirm the presence of L-DOPA in the polymer matrix of CuNP/MWCNT-MIP after rebinding process, CV of (a) GCE modified with CuNP/MWCNT-MIP and (b) NIP were recorded in 0.1 mol L^{-1} solution of PBS (pH 7.0) with potential ranging from −1000 to +1000 mV (Fig. 10) under N_2 atmosphere. Clear electro oxidation and reduction peaks appeared in the case of (a) whereas no such waves were observed in the other (b). In all cases the electrochemical measurements were carried out in template free PBS solution, which showed that the oxidation and reduction peaks showed by CuNPs/MWCNT-MIP modified GCE were solely due to the presence of embedded template molecules in the MIPs.

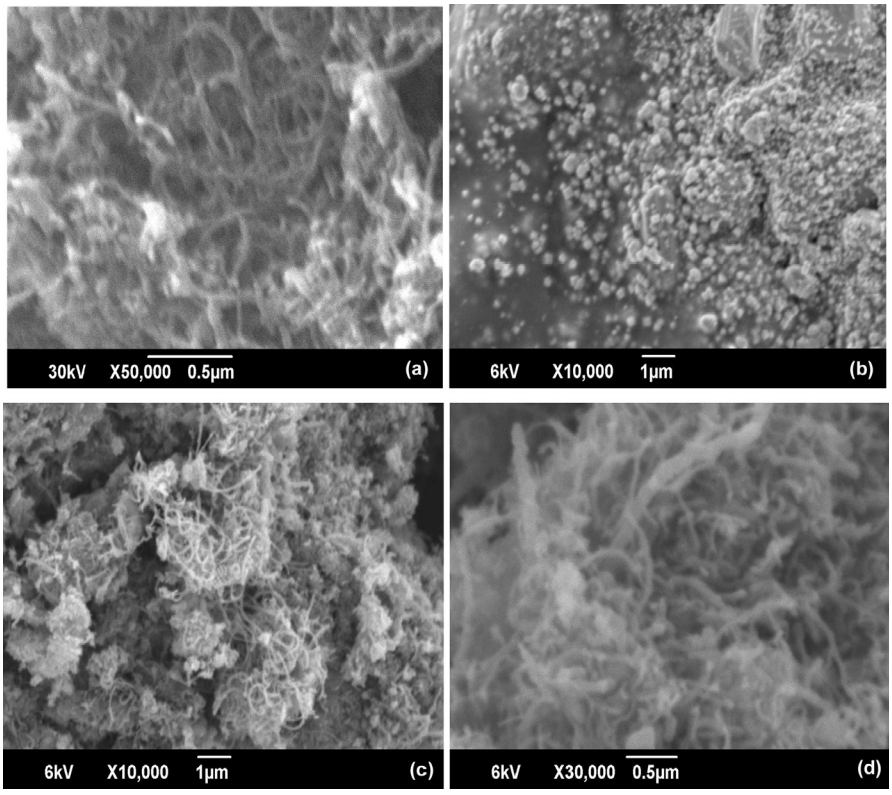

Fig. 5 Scanning electron micrographs of (a) MWCNT, (b) CuNP (c) CuNPs/MWCNT-CH═CH_2 (d) CuNPs/MWCNT-MIP.

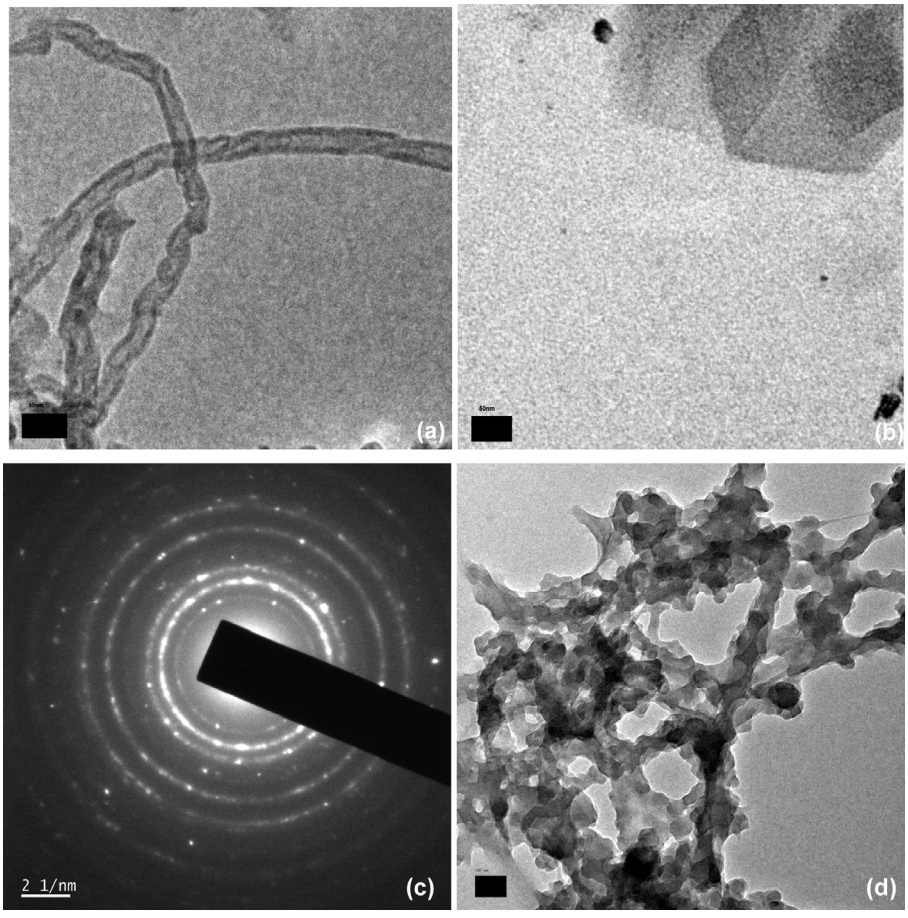

Fig. 6 TEM Images of (a) MWCNT (b) CuNPs (c) SAED image of CuNPs (d) CuNPs/MWCNT-MIP.

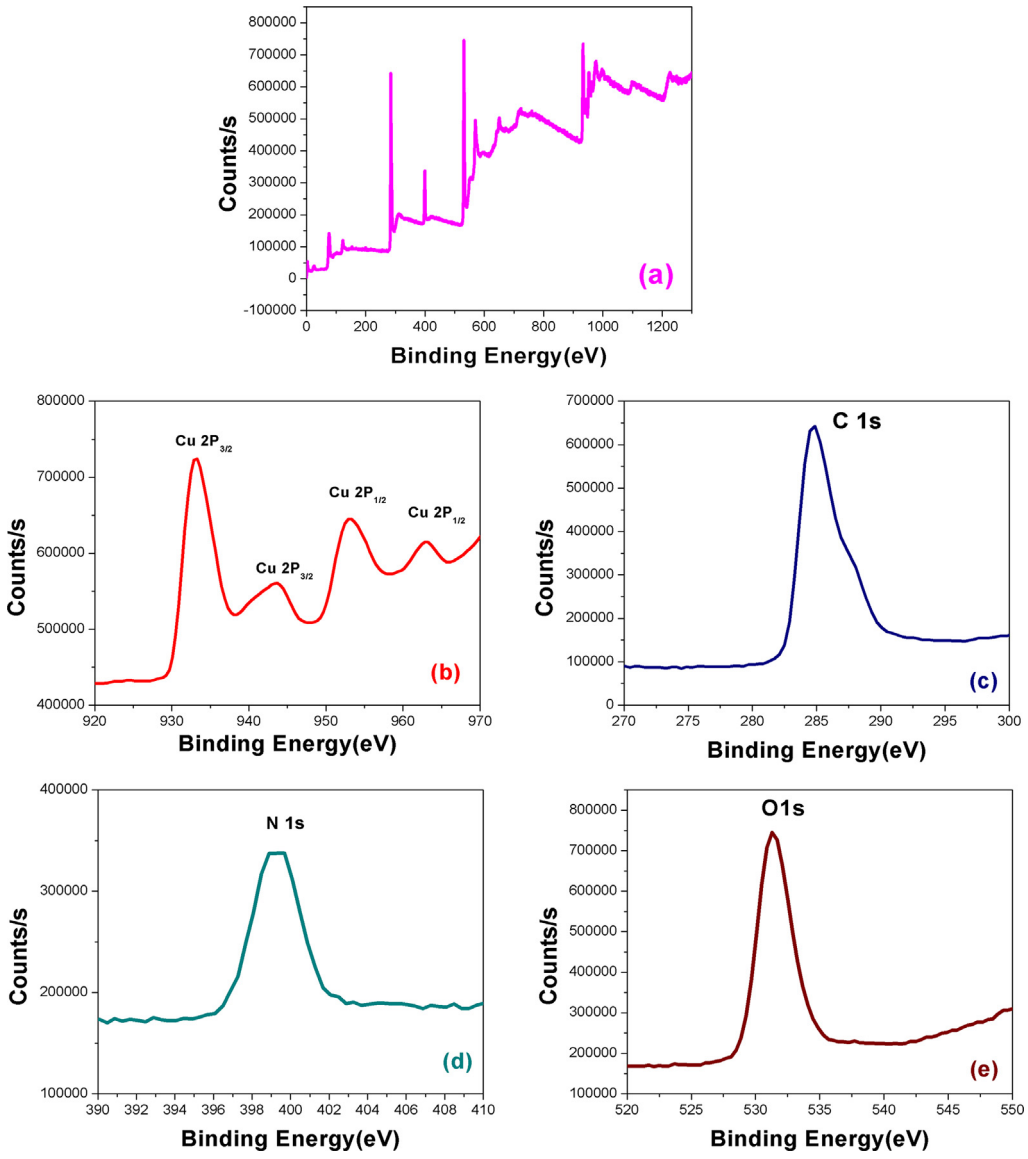

Fig. 7 XPS spectra of CuNPs/MWCNT-MIP (a), Cu 2p (b), C1s (c), N1s (d) and O1s (e).

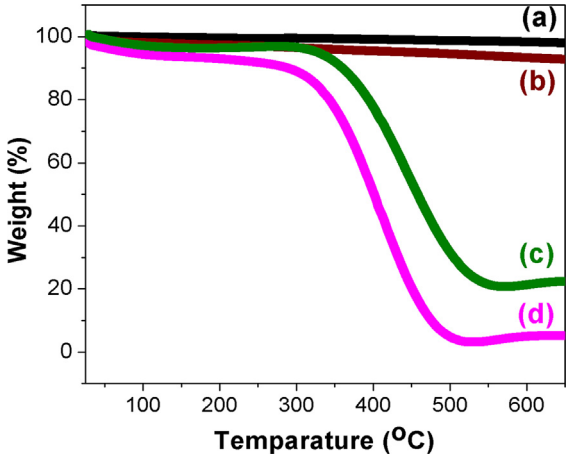

Fig. 8 Thermo gravimetric analysis curves of (a) MWCNT (b) MWCNT-CH=CH_2 (c) CuNPs/MWCNT-MIP and (d) conventional MIP (heating rate of 10 °C min^{-1} from room temperature to 700 °C under N_2 atmosphere).

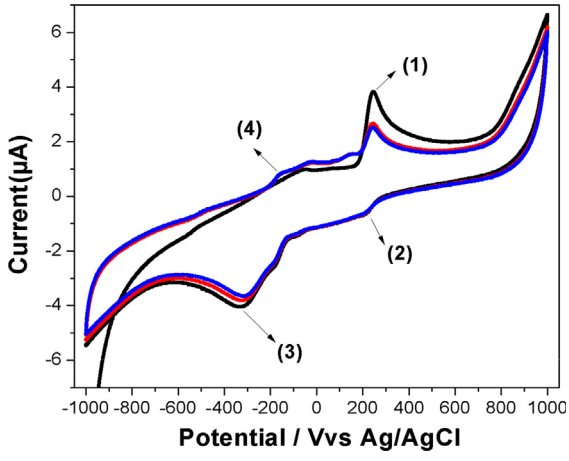

Fig. 9 Cyclic voltagrams obtained for CuNPs/MWCNT-MIP modified GCE in phosphate buffer (0.1 mmol L^{-1}, pH 7.0) containing 1×10^{-5} mol L^{-1} of L-DOPA. Scan rate: 100 mV s^{-1}; electrode area: 0.071 cm^2.

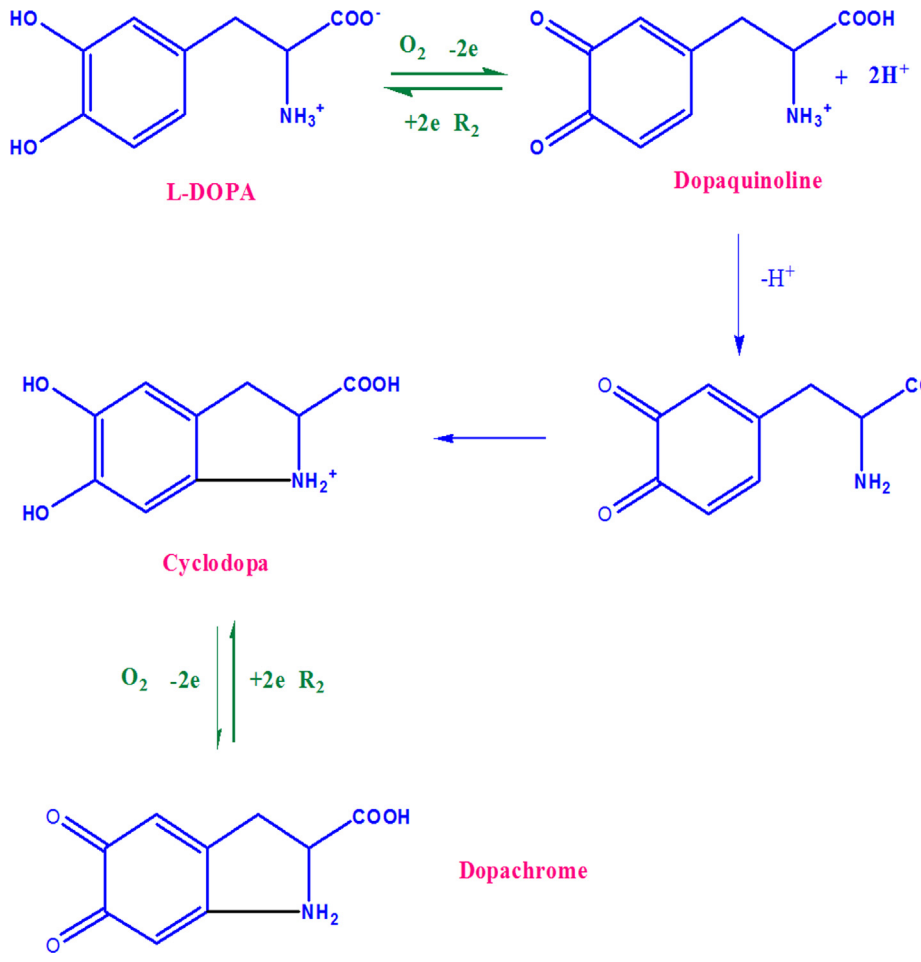

Scheme 3 The electrode mechanism of L-DOPA at CuNP/MWCNT-MIP modified GCE.

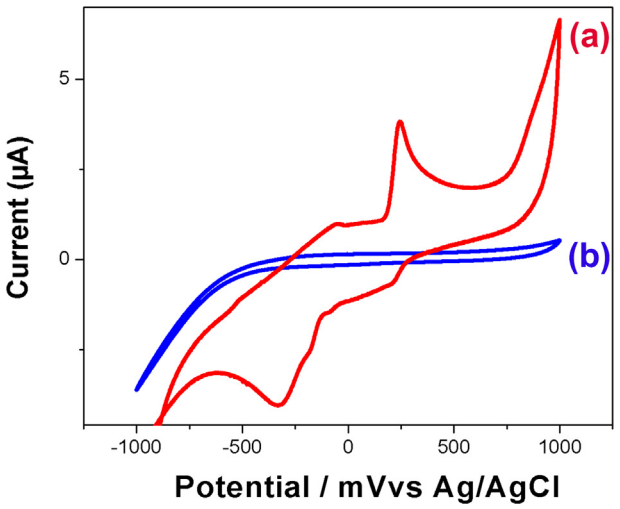

Fig. 10 Cyclic voltagrams obtained for (a) CuNPs/MWCNT-MIP and (b) CuNP/MWCNT-NIP modified GCEs in phosphate buffer (0.1 mmol L^{-1}, pH 7.0) containing 1×10^{-5} mol L^{-1} of LDOPA. Scan rate: 100 mV s^{-1}; electrode area: 0.071 cm^2.

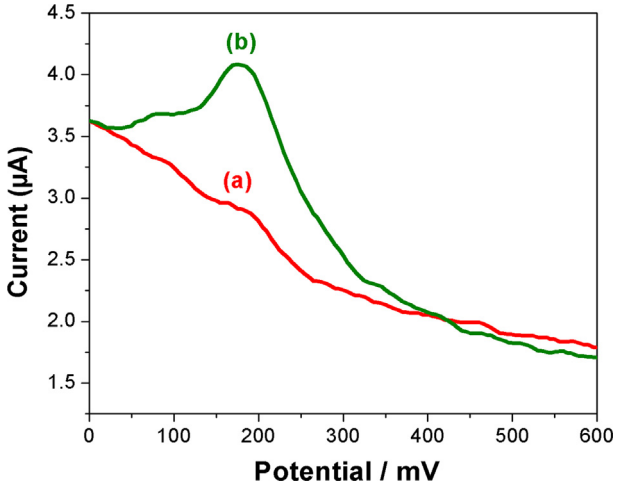

Fig. 11 Differential pulse voltagrams of CuNPs/MWCNT-NIP (a) and CuNPs/MWCNT-MIP sorbents modified GCE (b) in PBS buffer (pH 7) after incubation and shaking in 1×10^{-5} mol L^{-1} L-DOPA solution for 9 min with a scan rate of 20 mV s^{-1}, a pulse amplitude 50 mV, and a pulse width of 50 ms.

The rebinding ability of the imprinted sorbents was also monitored using DPV techniques by comparing the current response between imprinted and non imprinted sorbent modified GCE. Fig. 11 shows the difference in DPV response of (a) non imprinted sorbent modified GCE and (b) L-DOPA imprinted nanosorbent modified GCE in PBS after incubation

in 1×10^{-5} mol L^{-1} solution of L-DOPA about 10 min. The DPV response of CuNPs/MWCNT-MIP modified GCE is almost 1.4 times enhanced than that of the GCE. The results suggest the presence of more specific template recognition cavities in the imprinted polymer.

3.3. Optimization of the electrochemical sensor

3.3.1. Effect of pH

The pH value of supporting electrolyte is an important parameter affecting the sensing capacity of an electrochemical sensor. The CuNPs/MWCNT-MIPs modified GCE was employed for the investigation of the effect of pH the of phosphate buffer solution on sensing. Fig. 12 shows the variation on I (μA) with varying pH (4.0–10.0) at a fixed concentration of 1×10^{-5} mol L^{-1} L-DOPA for 10 min incubation time. The result shows that with increase in pH the current response of CuNPs/MWCNT-MIPs modified electrode also increases gradually. However, after reaching pH 7 current response decreases with increase in pH upto 10.0. The result obtained shows that current response was maximum at pH 7 for the CuNPs/MWCNT-MIPs modified GCE and hence was chosen as the optimized pH for further studies. In the optimal pH condition, L-DOPA is better inserted into the recognition cavities of the nano sorbent and thus better non covalent interactions are achieved.

3.3.2. Effect of time of incubation

The recognition kinetics of the surface modified GCE sensor towards the template was studied using DPV in 1×10^{-6} mol L^{-1} solution of L-DOPA (Fig. 13). The result shows that the current response increased suddenly up to 2.5 μA within the first 5 min, and then the increase in current response was to a much lesser extent. This suggests that uptake was rapid in the initial 5 min (90%) and the adsorption equilibrium was achieved within 9 min. The nanodimension of MIP and increase in surface to volume ratio made the recognition cavities more accessible for the template rebinding. The fast uptake kinetics of CuNPs/MWCNT-MIP modified GCE is an advantage for its analytical applications.

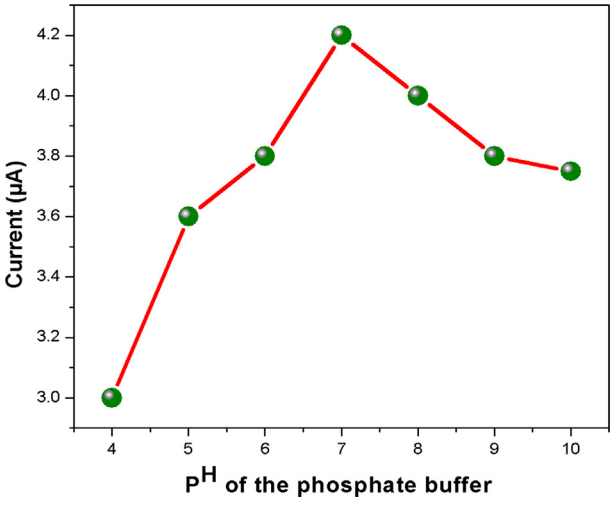

Fig. 12 The relationship between current response and pH value in 0.1 M phosphate buffer in the pH range of 4–10 at scan rate of 20 mV/s.

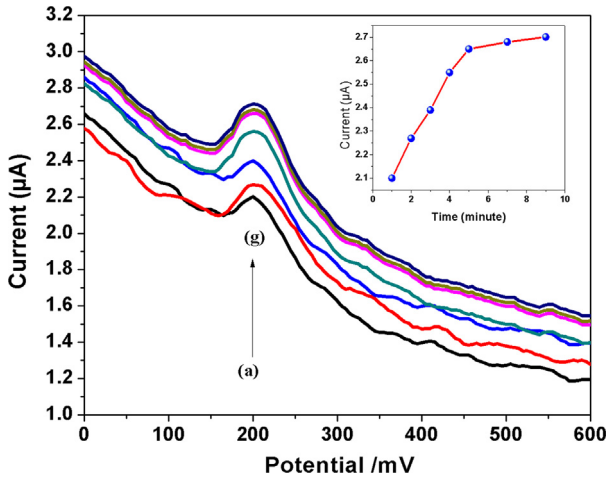

Fig. 13 DPV response with incubation time: 1, 2, 3, 4, 5, 7 and 9 min (a-g) in 0.1 mmol L^{-1} PBS (pH 7.0) with 1×10^{-6} mol L^{-1} L-DOPA by CuNPs/MWCNT-MIP sensor with a scan rate of 20 mV s^{-1}, a pulse amplitude 50 mV, and a pulse width of 50 ms. Inset: the uptake curve between time and peak current of DPV responses.

3.4. The concentration dependence, selectivity and reusability of the CuNPs/MWCNT-MIP modified electrode

The linearity of DPV response with respect to the template concentration ranging from 1×10^{-8} to 1×10^{-6} mol L^{-1} is given in Fig. 14. The linear regression equation is $i_p(\mu A) = 15.222C_{[DOPA]} + 2.66$, with a correlation coefficient of 0.9905 and a lower detection limit of 7.2323×10^{-9} mol L^{-1} (S/N = 3).

To evaluate the selectivity of the molecular imprinted polymer (CuNPs/MWCNT-MIP) modified sensor, differential pulse voltammetry was performed on structurally similar compound solutions (DA, UA, DOPAC and HVA) having

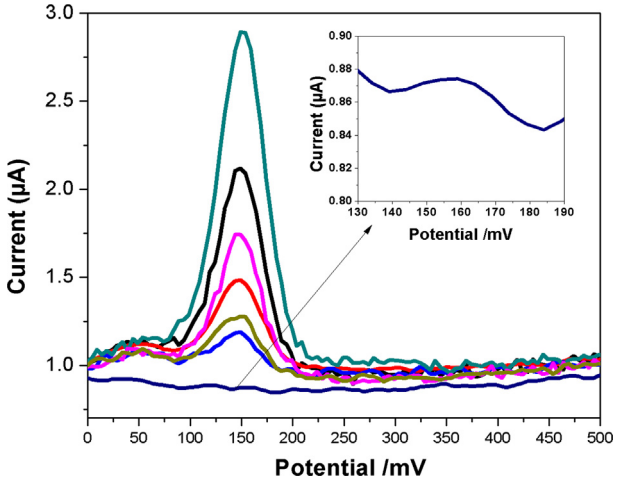

Fig. 14 The DPV current responses of CuNPs/MWCNT-MIP modified electrode (from a to g), after incubation (9 min) with different L-DOPA concentrations in 0.1 mmol L^{-1} PBS (pH 7.0) with a scan rate of 20 mV s^{-1}, a pulse amplitude 50 mV, and a pulse width of 50 ms. *Inset*: standard curve of L-DOPA, Concentration vs current.

same concentration. For this the MIP modified electrode was incubated in 0.1 mmol L^{-1} PBS containing 1×10^{-5} mol L^{-1} of template and each structural analogues for about 9 min. for the complete rebinding of analyte molecules and noted the DPV response (Fig. 15). The results show that DPV current response towards the template is maximum and almost 8 times more than that for the other two structural analogues

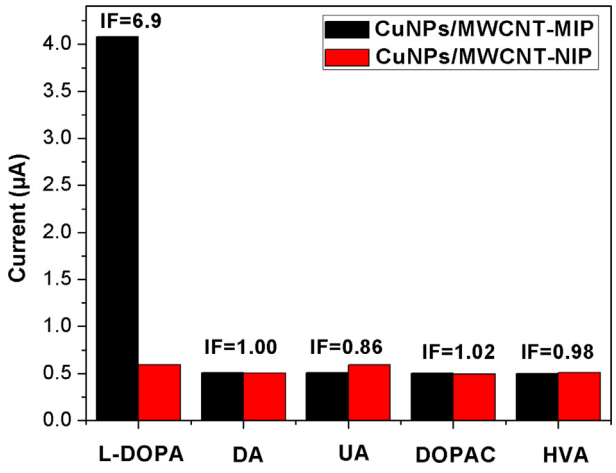

Fig. 15 Selective recognition of L-DOPA and its structurally related compounds by the CuNPs/MWCNT-MIP/NIPs modified GCE in 0.1 mmol L^{-1} PBS (pH 7.0) with 1×10^{-5} mol L^{-1} concentration of the corresponding chemical compounds.

but the adsorption capacity of NIP modified electrode is minimal and almost similar in all cases due to the lack of imprinted cavities.

The imprinting factor (IF) of the sensor towards L-DOPA is also calculated which confirms the specific recognition ability of CuNPs/MWCNT-MIP sensor.

$$\text{Imprinting factor IF} = [\text{Ip(MIP)}/\text{Ip(NIPs)}] \quad (1)$$

where Ip (MIP) is the current response of CuNPs/MWCNT-MIP to L-DOPA and Ip (NIPs) correspond to non imprinted sorbent. The high values of IF means the higher selectivity of CuNPs/MWCNT-MIP sorbent towards L-DOPA. The IF of L-DOPA is the maximum as compared to all other structural analogues which confirmes the maximum selectivity of CuNPs/MWCNT-MIP for L-DOPA. These result shows that the CuNPs/MWCNT-MIP modified GCE has very good recognition ability towards the template L-DOPA. The reusability of the MIP modified GCE was studied in 1×10^{-5} mol L^{-1} L-DOPA for 6 sequential cycles. The result gave an idea that the sensor shows reusability up to 6 cycles with a relative standard deviation (RSD) of 1.9%. In addition, the fabricated sensor retained its current response for 10 weeks.

3.5. Analytical application

The fabricated electrochemical sensor was successfully applied for the detection of L-DOPA in non-infected, infected human urine and pharmaceutical samples (Tables 1 and 2). The

Table 1 Comparison of cyclic voltammeric sensing capacity for the detection of L-DOPA by different materials.

Materials	Method	Concentration range (μ mol L^{-1})	Lower detection limit(μ mol L^{-1})	Reference
Chloro (pyridine) bis (dimethylglyoximato) cobalt(III)/multi-walled carbon nanotube	CV	3–100	0.86	Leite et al. (2012)
Cobalthexacyanoferrate /large mesopore carbon composite modified electrode	CV	0.1–1900	0.02	Yan et al. (2011)
Fe_3O_4 membrane	CV	0.05–10	0.01	Ali et al. (2014)
CuNPs/MWCNT-MIP	CV	0.01–1	0.009	Present work

Table 2 Determination of L-DOPA in urine and pharmaceutical samples by proposed method (N = 5).

Sample	Spiked value (μg)	Found value (μg)	Recovery (%)
Human urine	–	0.00	–
	10	9.89 ± 0.08	98.9
	25	24.86 ± 0.06	99.4
	50	50.90 ± 0.07	101.8
Infected Human urine	–	20.87 ± 0.10	–
	10	31.02 ± 0.12	100.1
	25	45.8 ± 0.09	99.7
	50	70.03 ± 0.11	98.3
Pharmaceutical sample	–	98.97 ± 1.02	–
	10[a]	109.09 ± 1.12	102.4
(L-DOPA tablet 100 mg)	25[a]	123.92 ± 1.29	99.8
	50[a]	149.83 ± 1.34	101.7

[a] The values are given in mg.

recovery of L-DOPA (between 98.3 and 102.4) and RSD obtained were acceptable. The highly satisfactory recovery of L-DOPA from the spiked non-infected and infected human urine samples and the good agreements between the experimental value (EV) and the original manufacturer's value (MV) for tablet indicated that the proposed method was good for practical sample analysis (MV was given as 100 mg tablet^{-1}). The sensor can thus provide a good alternative for the determination of
L-DOPA in real samples.

4. Conclusions

In the current work, a novel electrochemical sensor (CuNPs/MWCNT-MIP) for L-DOPA recognition has been developed. This method is found to be very sensitive with 7.230 nM detection limits for the monitoring of L-DOPA. Moreover, the synthesized CuNPs/MWCNT-MIP showed a highly specific recognition capability for L-DOPA over other structurally similar compounds, besides excellent stability and regeneration. Finally, the fabricated sensor was applied to the monitoring of L-DOPA in human urine and pharmaceutical samples and the results were satisfactory (Recovery percentage about 98.3–101.8). The current investigation suggests that CuNPs/MWCNT-MIP can act as a powerful sensor for the determination of L-DOPA in pharmaceutical and biological samples. The novel and simple strategy reported here can be further extended to quantify and qualify other electrochemically detectable template molecules as well.

References

Afkhami et al, 2013. Fabrication of a new electrochemical sensor based on a new nano-molecularly imprinted polymer for highly selective and sensitive determination of tramadol in human urine samples. Biosens. Bioelectron. 44, 34–40. https://doi.org/10.1016/j.bios.2012.11.030.

Ali, M. et al, 2014. Fluid interface-mediated nanoparticle membrane as an electrochemical sensor. RSC Adv. 4, 61404–61408. https://doi.org/10.1039/C4RA12149J.

Akhavan et al, 2011. CuO/Cu(OH)$_2$ hierarchical nanostructures as bactericidal photocatalystsm. J. Mater. Chem. 21, 9634–9640. https://doi.org/10.1039/C0JM04364H.

André et al, 2009. The formation of colloidal copper nanoparticles stabilized by zinc stearate: one-pot single-step synthesis and characterization of the core–shell particles. Phys. Chem. Chem. Phys. 11, 8358–8366. https://doi.org/10.1039/B908034A.

Annu, S. et al, 2012. Synthesis of copper nanoparticles in polycarbonate by ion implantation. Bull. Mater. Sci. 34, 645–649.

Ayesha, K. et al, 2016. A chemical reduction approach to the synthesis of copper nanoparticles. Int. Nano Lett. 1, 21–26. https://doi.org/10.1007/s40089-015-0163-6.

Bharat, K. et al, 2013. Enhanced hydrogen/oxygen evolution and stability of nanocrystalline (4–6 nm) copper particles. J. Mater. Chem. A. 1, 4728–4735. https://doi.org/10.1039/C3TA01194A.

Brooks, D.J., 2008. Optimizing levodopa therapy for Parkinson's disease with levodopa/carbidopa/entacapone: implications from a clinical and patient perspective. Neuropsychiatr. Dis. Treat. 4, 39–47.

Carstensen, J., 1990. Drug Stability. Principles and Practices. Marcel Dekker Inc, New York, USA.

Debart et al, 2001. A transmission electron microscopy study of the reactivity mechanism of Tailor-Made CuO particles toward lithium. J. Electrochem. Soc. 11, A1266–A1274.

Dhanani, T. et al, 2015. Comparison of green extraction methods with conventional extraction method for extract yield, L-DOPA concentration and antioxidant activity of Mucuna pruriens seed. Green Chem. Lett. Rev. 8, 43–48. https://doi.org/10.1080/17518253.2015.1075070.

Hyun, J. et al, 2015. Copper nanoparticle/multiwalled carbon nanotube composite films with high electrical conductivity and fatigue resistance fabricated via flash light sintering. ACS Appl. Mater. Interfaces. 7, 25413–25423. https://doi.org/10.1021/acsami.5b08112.

Jankovic, J., 2008. Parkinson's disease: clinical features and diagnosis. J. Neurol. Neurosurg. Psychiatry. 79, 368–376. https://doi.org/10.1136/jnnp.2007.131045.

Jungsup et al, 2017. Fabrication of sinter-free conductive Cu paste using sub-10 nm copper nanoparticles. J. Mater. Chem. C. 2017 (5), 12507–12512. https://doi.org/10.1039/C7TC02893H.

Kong, L. et al, 2012. An electrochemical sensor for rapid determination of ractopamine based on a molecularly imprinted electro synthesized o-aminothiophenol film. Anal. Bioanal. Chem. 404, 1653–1660. https://doi.org/10.1007/s00216-012-6253-7.

Kim, T. et al, 2007. Molecular dynamic simulation of heat pulse propagation in multiwall carbon nanotubes. Phys. Rev. B. 76, 155424. https://doi.org/10.1103/PhysRevB.76.155424.

Masooma, I. et al, 2015. An acid functionalized MWCNT/PVP nanocomposite as a new additive for fabrication of an ultrafiltration membrane with improved anti-fouling resistance. RSC Adv. 5, 95421–95432. https://doi.org/10.1039/C5RA11344J.

Mc, Evoy G., 2006. AHFS Drug Information. American Society of Health- System Pharmacists, Bethesda, USA.

Mc Murtrey, K. et al, 2000. HPLC resolution of the enantiomers of dihydroxyphenylalanine and selected salsolinol derivatives using sulfated beta-cyclodextrin. Enantiomer. 5, 377–383.

Menghe, M., 2011. Electrical conductivity of pure carbon nanotube yarns. Carbon 49, 3755–3761.

Mohamed, A.S. et al, 2017. Synthesis and characterization of multiwalled carbon nanotubes modified with octadecylamine and polyethylene glycol. Arabian J. Chem. 10, S921–S927. https://doi.org/10.1016/j.arabjc.2012.12.028.

Rashid, K. et al, 2012. On the aspect ratio effect of multi-walled carbon nanotube reinforcements on the mechanical properties of cementitious nanocomposites. Constr. Build. Mater. 35, 647–655. https://doi.org/10.1016/j.conbuildmat.2012.04.086.

Rike, Y. et al, 2011. Analysis of functional group sited on multi-wall carbon nanotube surface. Mater. Sci. J. 5, 242–247.

Roy, E. et al, 2014. A metronidazole-probe sensor based on imprinted biocompatible nanofilm for rapid and sensitive detection of anaerobic protozoan. RSC Adv. 4, 32881–32893. https://doi.org/10.1039/C4RA04868G.

Saleh, A. et al, 2009. Electrochemical sensors based on carbon nanotubes. Sensors 9, 2289–2319. https://doi.org/10.3390/s90402289.

Sukalyan, B. et al, 2008. One-pot copper nanoparticle-catalyzed synthesis of S-aryl- and S-vinyl dithiocarbamates in water: high diastereoselectivity achieved for vinyl dithiocarbamates. Green Chem. 10, 1224–1230. https://doi.org/10.1039/B809200A.

Sulekh, C. et al, 2014. Synthesis and characterization of copper nanoparticles by reducing agent. J. Saudi Chem. Soc. 18, 149–153. https://doi.org/10.1016/j.jscs.2011.06.009.

Török, R. et al, 2006. Enantioseparation of phenylalanine analogs on a quinine-based anion-exchanger chiral stationary phase: structure and temperature effects. J. Sep. Sci. 29, 2523–2532. https://doi.org/10.1002/jssc.200600100.

Vincenzo et al, 2009. Laser ablation synthesis in solution and size manipulation of noble metal nanoparticles. Phys. Chem. Chem. Phys. 11, 3805–3821. https://doi.org/10.1039/B900654K.

Wei, W.H. et al, 2007. Capillary electrophoresis-chemiluminecence detection of levodopa and benserazide in Medopar tablet. Chin. Chem. Lett. 18, 91–93. https://doi.org/10.1016/j.cclet.2006.11.034.

Leite, F.R.F. et al, 2012. Development of a sensor for L-Dopa based on $Co(DMG)_2ClPy$/multi-walled carbon nanotubes composite immobilized on basal plane pyrolytic graphite electrode. Bioelectrochemistry 86, 22–29. https://doi.org/10.1016/j.bioelechem.2012.01.001.

Yan, X. et al, 2011. Electrochemical determination of L-dopa at cobalt hexacyanoferrate/large-mesopore carbon composite modified electrode. J. Electroanal. Chem. 663, 36–42. https://doi.org/10.1016/j.jelechem.2011.09.024.

Yang, G. et al, 2014. Electrochemical determination of cefotaxime based on a three-dimensional molecularly imprinted film sensor. Biosens. Bioelectron. 53, 447–452. https://doi.org/10.1016/j.bios.2013.10.029.